



## PAPER

# Experimental validation of stochastic microdosimetric kinetic model for multi-ion therapy treatment planning with helium-, carbon-, oxygen-, and neon-ion beams

Taku Inaniwa<sup>1,3</sup>, Masao Suzuki<sup>2</sup>, Sung Hyun Lee<sup>1</sup>, Kota Mizushima<sup>1</sup>, Yoshiyuki Iwata<sup>1</sup>, Nobuyuki Kanematsu<sup>1</sup> and Toshiyuki Shirai<sup>1</sup>

<sup>1</sup> Department of Accelerator and Medical Physics, National Institute of Radiological Sciences, QST, 4-9-1 Anagawa, Inage-ku, Chiba 263-8555, Japan

<sup>2</sup> Department of Basic Medical Sciences for Radiation Damages, National Institute of Radiological Sciences, QST, 4-9-1 Anagawa, Inage-ku, Chiba 263-8555, Japan

<sup>3</sup> Author to whom any correspondence should be addressed.

E-mail: [inaniwa.taku@qst.go.jp](mailto:inaniwa.taku@qst.go.jp)

**Keywords:** charged-particle therapy, biological model, relative biological effectiveness, multi-ion therapy

Supplementary material for this article is available [online](#)

RECEIVED  
26 November 2019

REVISED  
15 January 2020

ACCEPTED FOR PUBLICATION  
22 January 2020

PUBLISHED  
12 February 2020

## Abstract

The National Institute of Radiological Sciences (NIRS) has initiated a development project for hypo-fractionated multi-ion therapy. In the treatment, heavy ions up to neon ions will be used as a primary beam, which is a high linear energy transfer (LET) radiation. The fractionated dose of the treatment will be 10 Gy or more. The microdosimetric kinetic (MK) model overestimates the biological effectiveness of high-LET and high-dose radiations. To address this issue, the stochastic microdosimetric kinetic (SMK) model has been developed as an extension of the MK model. By taking the stochastic nature of domain-specific and cell nucleus-specific energies into account, the SMK model could estimate the biological effectiveness of radiations with wide LET and dose ranges. Previously, the accuracy of the SMK model was examined by comparison of estimated and reported survival fractions of human cells exposed to pristine helium-, carbon-, and neon-ion beams. In this study, we verified the SMK model in treatment planning of scanned helium-, carbon-, oxygen-, and neon-ion beams as well as their combinations through the irradiations of human undifferentiated carcinoma and human pancreatic cancer cells. Treatment plans were made with the ion-species beams to achieve a uniform 10% survival of the cells within a cuboid target. The planned survival fractions were reasonably reproduced by the measured survival fractions in the whole region from the plateau to the fragment tail for all planned irradiations. The SMK model offers the accuracy and simplicity required in hypo-fractionated multi-ion therapy treatment planning.

## 1. Introduction

Carbon-ion radiotherapy has attracted growing interest due to its promising clinical results (Tsujii and Kamada 2012) originating from the increasing relative biological effectiveness (RBE) at the Bragg peak of carbon-ion beams as well as their advantageous depth-dose profile. Recently, several groups have investigated the potential of other ion beams, helium- (Krämer *et al* 2016, Tessonnier *et al* 2017a, 2017b), oxygen- (Kurz *et al* 2012, Sokol *et al* 2017, Tessonnier *et al* 2017a, 2017b), and neon-ion beams (Inaniwa and Kanematsu 2018) to effectively treat tumors with different radiation sensitivities against different ion species. In addition, the beam delivery of multiple ion species in a single treatment session has been investigated to maximize the therapeutic effects of charged-particle beams (Böhlen *et al* 2012, 2013, Krämer *et al* 2014, Inaniwa *et al* 2017). Hypo-fractionated treatments with high fractionated doses have also been investigated to reduce the patient burden caused by a prolonged treatment period (Miyamoto *et al* 2003, Kanai *et al* 2006, Tsujii and Kamada 2012). For further development of charged-particle therapy, we have initiated a development project for hypo-fractionated

multi-ion therapy. To practice the new treatment, the biological effectiveness of various ion species in wide ranges of linear energy transfer (LET) and dose has to be predicted for individual clinical cases based on biological models (Kanai *et al* 1999, Krämer and Scholz 2000, 2006, Inaniwa *et al* 2015b).

The microdosimetric kinetic (MK) model is a biological model to predict the biological effectiveness of radiations from the specific energy  $z_d$  absorbed by a microscopic subnuclear structure ‘domain’ (Hawkins 1994, 1996). By introducing the saturation correction to the domain-specific energy  $z_d$ , the MK model has been successfully used in clinical treatments of carbon-ion radiotherapy (Kase *et al* 2006, Inaniwa *et al* 2010, 2015b, Sato *et al* 2011). The MK model gives reasonable prediction of biological effectiveness for most clinical cases. However, when the model was applied to high-LET and high-dose radiations, it overestimated the biological effectiveness of the radiations (Sato and Furusawa 2012, Manganaro *et al* 2017, Chen *et al* 2018). In the MK model, the stochastic nature of domain-specific energy  $z_d$  is taken into account to predict the cell survival fraction, while the stochastic nature of the cell nucleus-specific energy  $z_n$  is ignored by assuming a constant value of  $z_n$  for all cell nuclei in a cell population, which is equivalent to the macroscopic dose  $D$  delivered to the population. Sato and Furusawa (2012) pointed out that the overestimation in biological effectiveness is induced by the intrinsic ignorance of the stochastic nature of  $z_n$  in the MK model. To address this issue, they numerically solved the fundamental equations of the MK model taking into account the stochastic nature of specific energies both in a domain  $z_d$  and a cell nucleus  $z_n$ , and named the procedure the stochastic microdosimetric kinetic (SMK) model. The SMK model-based calculation was accurate, but it was computationally intensive both in time and memory space requirements to deal with the stochastic natures in  $z_d$  and  $z_n$ , making the model difficult to use in daily clinical practice. Inaniwa and Kanematsu (2018) developed a computational method with a shorter computation time and a reduced memory space to calculate the biological effectiveness of charged particle beams based on the SMK model in treatment planning software. They evaluated the accuracy of the SMK model with the developed computational method by comparing the estimated and measured survival fractions of human salivary gland tumor (HSG) cells and V79 cells exposed to pristine helium-, carbon-, and neon-ion beams reported by Furusawa *et al* (2000).

In the present study, we verified the SMK model in treatment planning of helium-, carbon-, oxygen-, and neon-ion beams or combinations of them through cell irradiation experiments of two human cell lines for the hypo-fractionated multi-ion therapy.

## 2. Materials and methods

### 2.1. SMK model

In the SMK model, the survival fraction of cells  $S$  exposed to radiation of macroscopic dose  $D$  is predicted from the specific energy imparted to a domain  $z_d$ , the saturation-corrected specific energy imparted to a domain  $z'_d$ , and the specific energy imparted to a cell nucleus  $z_n$  by the radiation, taking stochastic natures of these quantities into account as

$$S(D) = \exp(-\alpha_{\text{SMK}}D - \beta_{\text{SMK}}D^2) \left[ 1 + D \left\{ -\beta_{\text{SMK}} + \frac{1}{2}(\alpha_{\text{SMK}} + 2\beta_{\text{SMK}}D)^2 \right\} \bar{z}_{n,D} \right] \quad (1)$$

with

$$\alpha_{\text{SMK}} \equiv (\alpha_0 + \bar{z}_{d,D}^* \beta_0) \quad (2)$$

and

$$\beta_{\text{SMK}} \equiv \beta_0 (\bar{z}_{d,D}^* / \bar{z}_{d,D}). \quad (3)$$

Inaniwa and Kanematsu (2018), where  $\alpha_0$  and  $\beta_0$  are  $\alpha$  and  $\beta$  parameters of the linear-quadratic model in the limit of LET = 0,  $\bar{z}_{d,D}$ ,  $\bar{z}_{d,D}^*$  and  $\bar{z}_{n,D}$  are the dose averaged values of  $z_d$ ,  $z'_d$  and  $z_n$  per event, respectively. The saturation-corrected domain-specific energy  $z'_d$  is given by

$$z'_d = \frac{z_0^2}{z_d} \left\{ 1 - \exp \left[ -(z_d/z_0)^2 \right] \right\} \quad (4)$$

with the saturation parameter  $z_0$  representing the decrease in the number of complex DNA damages per dose at the high-LET regions (Hada and Georgakilas 2008).

### 2.2. Setup for the SMK model-based treatment planning

#### 2.2.1. SMK model parameters

For the estimation of the cell survival fraction based on the SMK model, the following five parameters are requisites:  $\alpha_0$  in (2),  $\beta_0$  in (2) and (3), the saturation parameter  $z_0$  in (4), and the radii of domain  $r_d$  and cell nucleus  $R_n$ . The domain radius  $r_d$  is used to derive  $\bar{z}_{d,D}$  and  $\bar{z}_{d,D}^*$ , and the nucleus radius  $R_n$  is used to derive

$\bar{z}_{n,D}$ . These parameters depend only on the cell line, and they are independent of the radiation type. We assumed  $R_n = 8.1 \mu\text{m}$  for all human cell lines following our previous study (Inaniwa and Kanematsu 2018), while the other parameters were determined from measured cell survival curves in this study.

### 2.2.2. Cell irradiations

To determine the numerical values of  $\alpha_0$ ,  $\beta_0$ ,  $z_0$ , and  $r_d$ , we measured cell survival curves of two human cancer cells: human undifferentiated carcinoma cells from the mouth floor distributed by the JCRB Cell Bank in the National Institutes of Biomedical Innovation, Health and Nutrition (Cell name, HSGc-C5; Cell No., JCRB1070) and pancreatic cancer cells distributed by the RIKEN BioResource Center Cell Bank (Cell name, MIA PaCa-2; Cell No., RCB2094). The HSGc-C5 cells were cultured in Eagle's minimum essential medium (MEM) containing kanamycin ( $60 \text{ mg l}^{-1}$ ), supplemented with 10% fetal bovine serum (FBS, Lot# 160418-03, Equitech-Bio, Inc., Kerrville, TX) in an incubator at 5%  $\text{CO}_2$  and 37 °C. The MIA PaCa-2 cells were cultured in D-MEM (High Glucose) with L-glutamine, phenol red and sodium pyruvate (043-30085, FUJIFILM Wako Pure Chemical Corporation, Osaka, Japan), supplemented with 10% fetal bovine serum (FBS, Gibco Lot# 42F3483K, Thermo Fisher Scientific, Waltham, MA) and 1% of penicillin-streptomycin solution ( $\times 100$ ) (168-23191, FUJIFILM Wako Pure Chemical Corporation, Osaka, Japan) in an incubator at 5%  $\text{CO}_2$  and 37 °C.

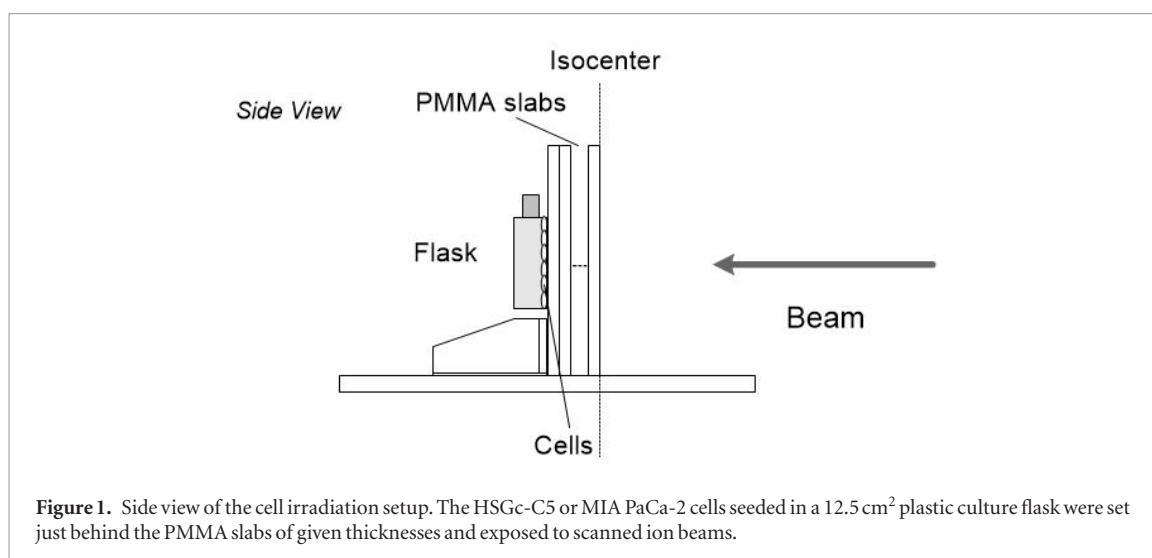
Both cells obtained in a frozen vial from the cell bank were thawed out and sub-cultured twice in a 75  $\text{cm}^2$  plastic culture flask (Cell Culture Flask, Falcon 353135, Corning Inc., Corning, NY) at a density of  $10^6$  per flask. The expanded stock culture was frozen and subdivided into polypropylene vials (Wheaton 985731, Millville, NJ) in liquid nitrogen until use. The frozen stocked cells were thawed in a water bath at 37 °C for irradiation, then inoculated and subcultured in the 75  $\text{cm}^2$  plastic flask until they reached a confluent state. The following day, the cells were trypsinized and subcultured again onto 12.5  $\text{cm}^2$  plastic culture flasks (Cell Culture Flask, Falcon 353018, Corning Inc.) at a density of  $2 \times 10^6$  cells per dish 2 ds before irradiation. The plating efficiencies of the cells for colony formation on a 60 mm or 100 mm plastic dish (Tissue Culture Dish, Falcon 353001 or 353003, Corning Inc.) were around 80% for HSGc-C5 cells and 60% for MIA PaCa-2 cells.

All cell irradiation experiments were performed using the pencil beam scanning system at the NIRS (Furukawa *et al* 2010). Figure 1 shows the experimental setup. The 12.5  $\text{cm}^2$  plastic culture flasks were set behind polymethyl methacrylate (PMMA) slabs of given thicknesses. Pristine helium-, carbon-, oxygen-, and neon-ion beams were scanned perpendicularly to make a uniform square field of  $10 \times 10 \text{ cm}^2$  at the isocenter plane to sufficiently cover the flasks. The dose-averaged LET of each ion-species beam at the cell sample was adjusted at four or five different values by changing the beam energy and thickness of the PMMA slab up to 4 mm. These LET values were determined by a Geant4-based Monte Carlo simulation (Agostinelli *et al* 2003) of the beams impinging on a PMMA phantom at the corresponding residual ranges in PMMA. The dose-averaged LET was used as an index of spectrum information of the radiations, though the quantity dose not accurately link to the biological effectiveness of the radiations (Grün *et al* 2019). For each ion species and LET, delivered dose levels were varied from 0.5 Gy to 5 Gy to measure the survival curves for the cells. The applied dose was controlled with a dose monitor of the irradiation system, which was calibrated against the calibrated Markus ion chamber (Type 34045, PTW, Freiburg, Germany) for each ion species and LET. The wall thickness of the Markus ion chamber was adjusted to 1.0 mm in PMMA, which equals to the PMMA-equivalent thickness of the 12.5  $\text{cm}^2$  plastic culture flask.

All cell irradiation experiments for determining the SMK model parameters were performed once. Within 30 min after the irradiations, the cells were rinsed with phosphate buffered saline, trypsinized and then a suitable number of cells was plated onto 6 cm-diameter plastic culture dishes (Cell Culture Dish, Falcon 353002, Corning Inc.) to make 60–70 colonies per dish. The colonies were fixed and stained with 20% methanol and 0.2% crystal violet after a 14 d incubation in an incubator at 5%  $\text{CO}_2$  and 37 °C. Three replicate dishes were seeded for each data point and colonies consisting of more than 50 cells were scored as survivors.

### 2.2.3. Determination of the SMK model parameters

To estimate the survival fractions of the HSGc-C5 and MIA PaCa-2 cells for the experiments with the pristine beams, we followed the computation procedures described elsewhere (Inaniwa *et al* 2010, Inaniwa and Kanematsu 2018). The sensitive volumes of the domain and cell nucleus were assumed as cylinders of water with radii  $r_d$  and  $R_n$ , and lengths  $2r_d$  and  $2R_n$ , respectively. The incident ions traversed through the sensitive volumes along the direction parallel to the cylindrical axis. The radial dose distribution around the trajectory of the ions with the LET was described by the Kiefer-Chatterjee amorphous track structure model (Chatterjee and Schaefer 1976, Kiefer and Straaten 1986, Kase *et al* 2006). The specific energy deposited in a single event was an energy deposition in the sensitive volume from an ion track. For simplicity, we assumed a monoenergetic spectrum of helium-, carbon-, oxygen-, and neon-ion beams with the estimated LETs, unlike the actual experiments where the PMMA slabs of  $\leq 4$  mm in thickness were used to adjust the LETs. Under an assumption of a uniform distribution for the ion traversal through the sensitive volumes, we determined  $\bar{z}_{d,D}$ ,  $\bar{z}_{d,D}^*$ , and  $\bar{z}_{n,D}$  absorbed by the domain and nucleus for the radiations. Then, for given SMK model parameters  $\alpha_0$ ,  $\beta_0$ ,  $z_0$ ,  $r_d$ , and  $R_n$ , the



survival fraction of the cells exposed to the pristine beams of the four ion species could be estimated based on the SMK model with (1).

The SMK model parameters for each cell line were determined by minimizing the total square deviation of  $\log_{10}S$

$$\chi^2 = \sum_{i=1}^n [\log_{10}(S_{m,i}) - \log_{10}(S_{e,i})]^2 \quad (5)$$

by changing the SMK model parameters other than  $R_n$  in a step-by-step manner, where  $S_{m,i}$  and  $S_{e,i}$  are the measured and estimated survival fractions under the  $i$ th irradiation condition specified by the ion species, LET, and dose level, and  $n = 100$  and  $80$  were the numbers of data points in the cell irradiation experiments used in the least squares regression for the HSGc-C5 and MIA PaCa-2 cell lines, respectively. The parameter values of  $\alpha_0$ ,  $\beta_0$ ,  $z_0$ , and  $r_d$  were changed in  $0.001 \text{ Gy}^{-1}$ ,  $0.0001 \text{ Gy}^{-2}$ ,  $0.1 \text{ Gy}$ , and  $0.01 \mu\text{m}$  steps, respectively, to achieve the best fit to the measured survival fractions.

#### 2.2.4. Beam modeling for SMK model based treatment planning

For SMK model based treatment planning, we generated pencil beam data for helium-, carbon-, oxygen-, and neon-ion beams for the HSGc-C5 and MIA PaCa-2 cells using the determined SMK-model parameters in 2.2.3. In the pencil beam scanning (Haberer *et al* 1993), the Bragg peak of a narrow pencil beam is delivered to positions, referred to as ‘spots’, across the target volume with varying spot weights. To calculate the cell survival distribution in patient by charged-particle therapy treatment planning, distributions of dose,  $\bar{z}_{d,D}$ ,  $\bar{z}_{d,D}^*$ , and  $\bar{z}_{n,D}$  of the pencil beam delivered to the spots (beamlets) have to be calculated. In our treatment planning software, the distributions of dose,  $\bar{z}_{d,D}$ ,  $\bar{z}_{d,D}^*$ , and  $\bar{z}_{n,D}$  for pencil beams in water were predetermined with the dose measurements combined with the Monte Carlo simulations for particle spectrum distribution and the Kiefer–Chatterjee track structure model for radial dose distribution around the trajectory of the particles (Inaniwa *et al* 2010, 2014, Inaniwa and Kanematsu 2018). The distributions in water were then modeled with the triple-Gaussian trichrome model (Inaniwa and Kanematsu 2015), and registered in the software as pencil beam data. The data are used for the calculations in patients with density scaling using stopping power ratio of body tissues to water to calculate the distributions of dose,  $\bar{z}_{d,D}^*$ ,  $\bar{z}_{d,D}$ , and  $\bar{z}_{n,D}$  of the beamlets in each treatment plan (Inaniwa and Kanematsu 2018).

### 2.3. Cell irradiations for validation of the SMK model

For the validation of the SMK model, single- and multi-ion beams treatment plans were made with the in-house treatment planning software for scanned charged-particle therapy (Inaniwa and Kanematsu 2018).

#### 2.3.1. Cell irradiations with single-ion beams

To verify the SMK model in charged-particle therapy treatment planning of helium-, carbon-, oxygen-, and neon-ion beams, we performed cell irradiation experiments using the pencil beam data generated in 2.2.4. We defined a cuboid target of  $10 \times 10 \times 6 \text{ cm}^3$  centered at  $11.6 \text{ cm}$  depth in a PMMA phantom. The survival fraction of 10% for the HSGc-C5 and MIA PaCa-2 cells was prescribed to the target with helium-, carbon-, oxygen-, and neon-ion beams. The spots were arranged on regular grids of  $3 \text{ mm}$  spacing, which covered the target volume with adequate margins for lateral and distal falloffs. The number of ions delivered to each spot (spot weight) was

determined by the optimization algorithm of the treatment planning software (Inaniwa *et al* 2014, Inaniwa and Kanematsu 2015, 2018). For the dose calculations, the dose calculation errors due to water-nonequivalence of the PMMA in inelastic nuclear interactions were accounted for by the dedicated correction method (Inaniwa *et al* 2015a, 2020).

The cell culturing methods and experimental setup were the same as those described in 2.2.2. The thickness of the PMMA slabs upstream from the 12.5 cm<sup>2</sup> plastic culture flask was varied to adjust the depth for the cell irradiation within the irradiation field. For depth-survival curve measurements, we chose 12 different depths including six depths in the target volume. All depth-survival curve measurements were repeated twice on different days. The irradiation time for each field was 1–3 min.

### 2.3.2. Cell irradiations with multi-ion beams

To verify the SMK model in multi-ion therapy treatment planning, we made treatment plans of helium- and oxygen-ion beams and of carbon- and neon-ion beams. The survival fraction of 10% for the HSGc-C5 and MIA PaCa-2 cells was prescribed to the same target in the PMMA phantom.

In the treatment plans for the HSGc-C5 cells, two ion-species fields were designed sequentially as follows: (a) the first field was designed with the helium- (carbon-) ion beam to obtain a survival fraction of 41.6% corresponding to x-ray dose of 2.40 Gy within the target, and (b) the second field was designed with the oxygen- (neon-) ion beam superposed on the first field to obtain the cumulative survival of 10.0% corresponding to x-ray dose of 4.80 Gy within the target. The survival curve of the HSGc-C5 cells exposed to a 200 kVp x-ray is shown in supplemental figure S1 (available at [stacks.iop.org/PMB/65/045005/mmedia](https://stacks.iop.org/PMB/65/045005/mmedia)). During the spot-weights optimization of the second field, the spot weights of the first field were fixed. This dose prescription procedure including the half-dose prescription to the first field follows clinical practice of carbon-ion radiotherapy in multiple-fields sessions. Two ion-species fields were designed sequentially as well in the treatment plans for the MIA PaCa-2 cells with the prescribed survival levels in the target of 55.9% for the first field and the cumulative prescribed survival of 10.0% for the second fields, respectively, corresponding to x-ray doses of 2.19 and 4.37 Gy. The survival curve of the MIA PaCa-2 cells exposed to a 200 kVp x-ray is shown in supplemental figure S2. The time interval between the first and the second field irradiations was within 30 min for all plans. The temperature around the cells was 25 °C ± 1.5 °C during the experiments. The effect of sub-lethal damage repair during the experiment on the cell survival fraction should be insignificant (Inaniwa *et al* 2013).

By setting a Markus ion chamber behind the PMMA slabs, we measured the depth-dose distributions along the central beam axis for all the irradiation fields.

## 3. Results

### 3.1. Determination of the SMK model parameters

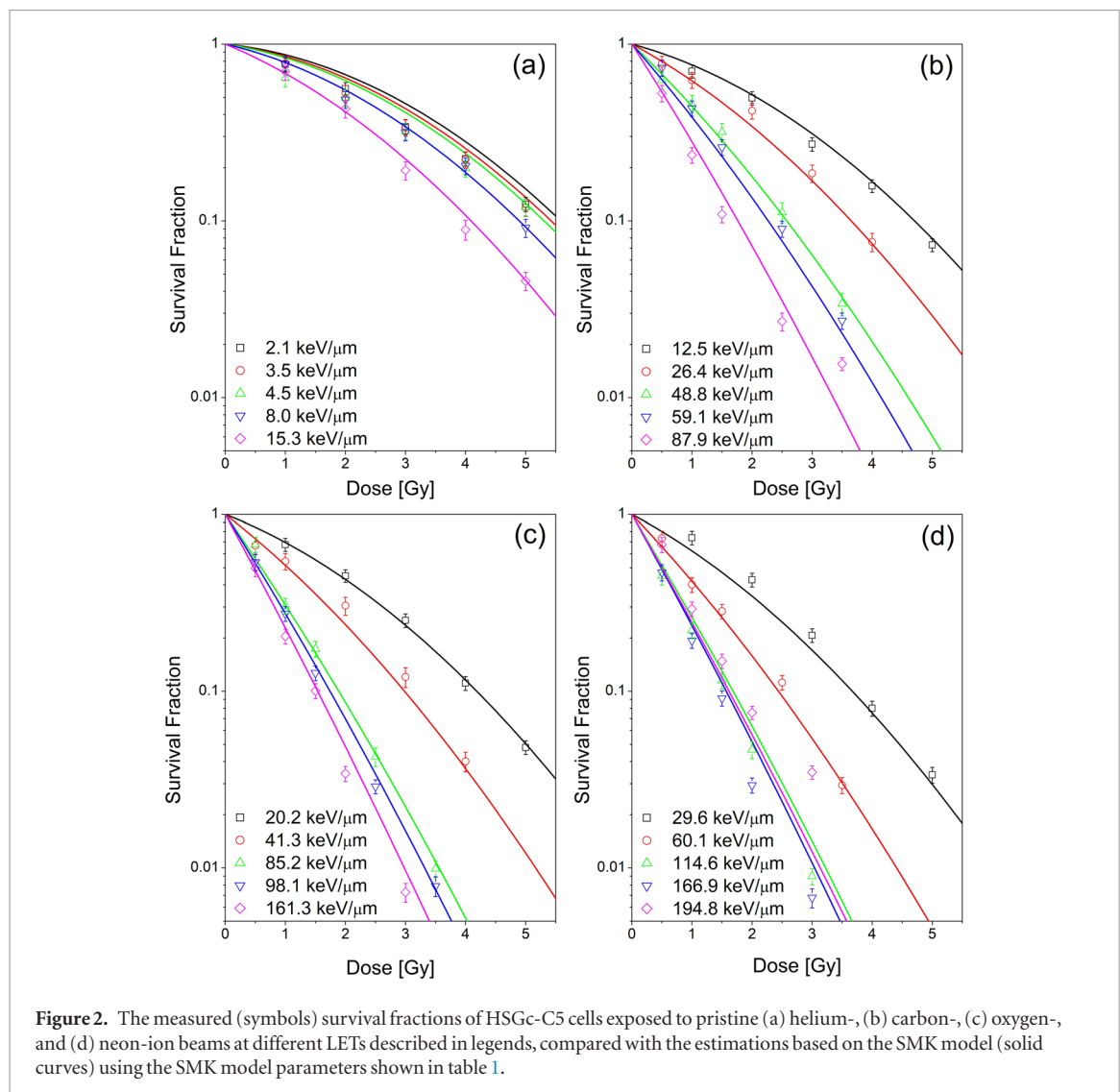
Figures 2 and 3 show the measured survival fractions of the HSGc-C5 and MIA PaCa-2 cells exposed to pristine helium-, carbon-, oxygen-, and neon-ion beams at different LETs. For the beams with LET  $\lesssim 160$  keV  $\mu\text{m}^{-1}$ , the higher the LET of the beams, the lower the survival fraction was at a given dose level for both cell lines. For the beams with LET  $\gtrsim 160$  keV  $\mu\text{m}^{-1}$ , however, the survival fraction at a given dose turned upwards to higher values due to the overkill effect. The variation in the dose response with LET was larger for the HSGc-C5 cells compared to the variation for the MIA PaCa-2 cells.

Table 1 shows the SMK model parameters determined to reproduce the measured cell survival fractions for the HSGc-C5 and MIA PaCa-2 cells. The values of the determined parameters differed greatly between the two cell lines. Figures 2 and 3 also show the estimated cell survival fractions using the SMK model parameters of the table for the HSGc-C5 and MIA PaCa-2 cells, respectively. For both cell lines, the SMK model reproduced the measured cell survival fractions with reasonable accuracy over wide dose and LET ranges for all ion species.

### 3.2. Validation of the SMK model

#### 3.2.1. Cell irradiations with single-ion beam

Figure 4 shows the comparisons between the measured and planned survival profiles of the HSGc-C5 cells as a function of depth in PMMA phantom exposed to the cuboid fields of helium-, carbon-, oxygen-, and neon-ion beams. The planned survival profiles were reproduced by the measured survival fractions in the whole region from the plateau to the fragment tail. The average values of measured survival fractions within the target were 10.3%, 10.0%, 10.1%, and 10.1% for helium-, carbon-, oxygen-, and neon-ion beams, respectively. These values corresponded to the x-ray doses of 4.76, 4.80, 4.79, and 4.79 Gy, respectively, for the HSGc-C5 cells. The measured dose profiles for the fields of HSGc-C5-cell irradiations are shown in supplemental figures S3–S6, respectively. Figure 5 shows the comparisons between the measured and planned survival profiles of the MIA PaCa-2 cells. The average values of measured survival fractions within the target were 10.4%, 10.3%, 10.4%, and 10.5% for the ion-species beams, which corresponded to x-ray doses of 4.33, 4.34, 4.33, and 4.32 Gy, respectively, for



the MIA PaCa-2 cells. The measured dose profiles for the fields of MIA PaCa-2-cell irradiations are shown in supplemental figures S7–S10, respectively. A systematic underestimation in survival fractions was observed at the plateau region of the neon-ion field. The planned survival fraction at the entrance was 19.3% (x-ray dose of 3.69 Gy), while the measured survival fraction at the position was 23.3% (x-ray dose of 3.47 Gy).

### 3.2.2. Cell irradiations with multi-ion beam

The measured survival profiles of the HSGc-C5 and MIA PaCa-2 cells exposed to the multi-ion beams are shown in figures 6 and 7, respectively, as a function of depth in PMMA phantom, along with the dose profiles of the constituent ion-species beams. The planned dose profiles were reproduced by the measured dose profiles in PMMA phantom within an accuracy of 1.5% in the whole region for all ion-species fields owing to the nuclear interaction correction methods developed and validated for helium-, carbon-, oxygen-, and neon-ion beams (Inaniwa *et al* 2015a, 2020). The planned survival profiles were also reproduced by the measured survival profiles in the whole region for both multi-ion plans and for both cell lines. For the HSGc-C5 cells (figure 6), the average values of measured survival fractions within the target were 10.2% and 10.0% for the helium-and-oxygen and carbon-and-neon ion plans, which corresponded to x-ray doses of 4.77 and 4.80 Gy, respectively. For the MIA PaCa-2 cells (figure 7), the average values of measured survival fractions within the target were 10.2% and 10.3% for the helium-and-oxygen and carbon-and-neon ion plans, which corresponded to x-ray doses of 4.35 and 4.34 Gy, respectively. The reproducibility of the survival profiles measured on different days was high especially for the HSGc-C5 cells.

## 4. Discussion

The SMK model for charged-particle therapy treatment planning with helium-, carbon-, oxygen-, and neon-ion beams was verified through the cell irradiation experiments of two human cell lines. By optimally determining the SMK model parameters, the survival fractions of the cells exposed to the pristine beams at different LETs

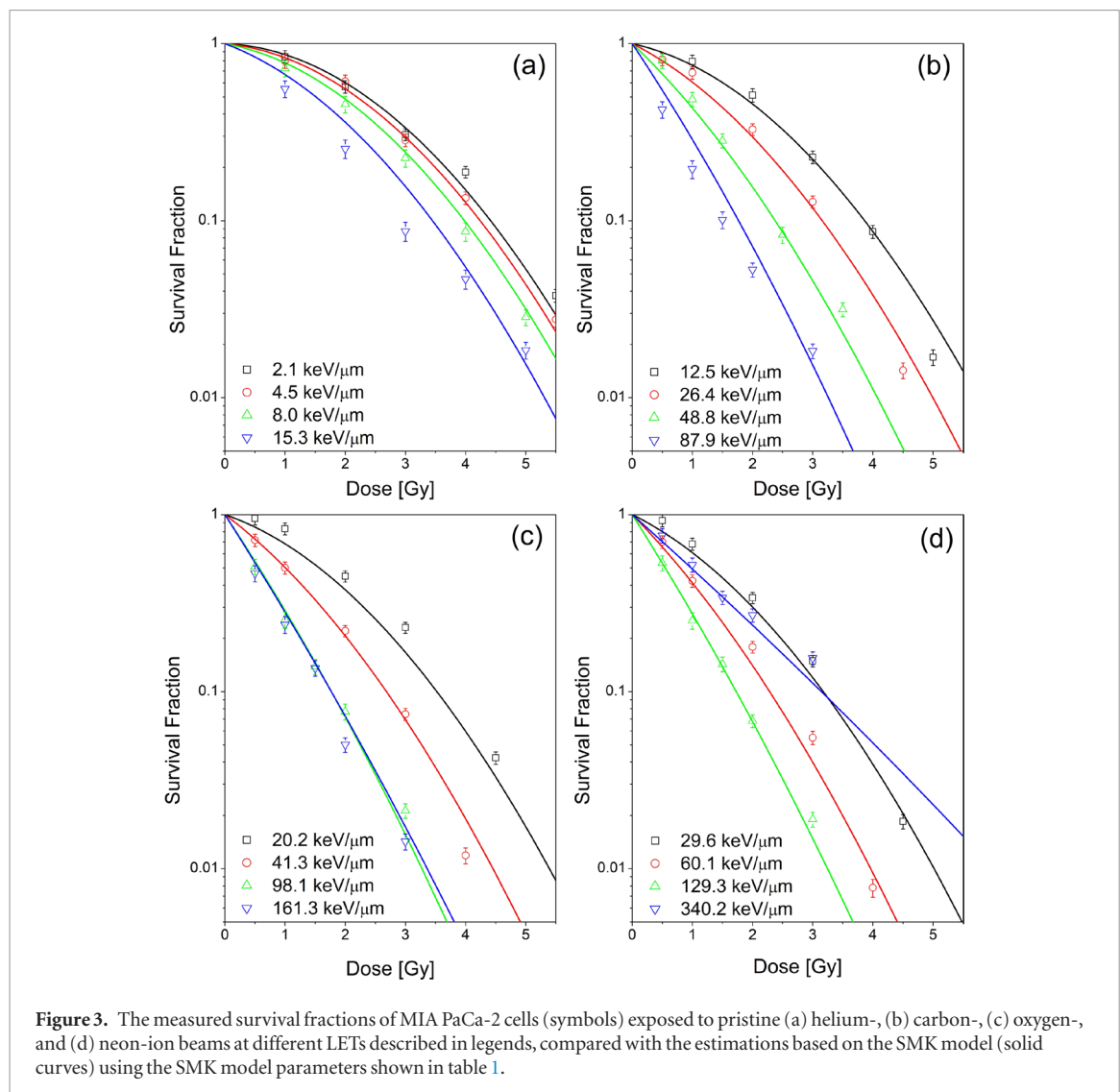


**Table 1.** The SMK model parameters determined from the least-square fitting of the measured cell survival fractions of the HSGc-C5 and MIA PaCa-2 cells exposed to pristine helium-, carbon-, oxygen-, and neon-ion beams at different LETs. The radius of the cell nucleus,  $R_n$ , was assumed to be  $8.1 \mu\text{m}$  for both human cell lines.

Cell line	$\alpha_0 \text{ (Gy}^{-1}\text{)}$	$\beta_0 \text{ (Gy}^{-2}\text{)}$	$z_0 \text{ (Gy)}$	$r_d \text{ (}\mu\text{m)}$
HSGc-C5	0.051	0.0564	53.0	0.34
MIA PaCa-2	0.001	0.1067	24.0	0.46

could be estimated in wide ranges of dose. The utilized human cell lines, the HSGc-C5 and MIA PaCa-2 cells, represented largely different radiation sensitivities. They are considered as two extreme human cell lines. Thus, the SMK model should be applicable to predict survival fractions of most human cells exposed to the radiations with wide LET and dose ranges. Treatment plans were made with the single-ion beams or combinations of the beams of two ion species to achieve a 10% survival of the cells within a cuboid target in a PMMA phantom. The planned survival distributions to a cuboid target in the PMMA phantom were reasonably reproduced by the measured cell survival fractions for all treatment plans. A small but systematic underestimation in survival fractions was observed at the plateau region of the neon-ion field for MIA PaCa-2 cells (figure 5(d)). The effect due to not correcting the parameter  $R_n$  for radiosensitivity by assuming a constant value of  $8.1 \mu\text{m}$  might be a reason for this observed underestimation. Inaccuracy of the SMK model parameters as well as that of the track structure model assumed in this study might be other reasons. The limitation of the SMK model might possibly be another reason. The investigation of the reasons is a task for the future.

The SMK model parameters determined for the HSGc-C5 cells in this study were different from the parameters determined previously (Inaniwa and Kanematsu 2018) for HSG cells using the reported cell survival fractions by Furusawa *et al* (2000):  $\alpha_0 = 0.174 \text{ Gy}^{-1}$ ,  $\beta_0 = 0.0568 \text{ Gy}^{-2}$ ,  $z_0 = 66.0 \text{ Gy}$ , and  $r_d = 0.28 \mu\text{m}$ . This discrepancy in parameter values might be due to the change in radiosensitivity of the HSG cell line over time. For example, the 10% survival dose of HSG cells for 200 kVp x-rays measured by Furusawa *et al* (2000)

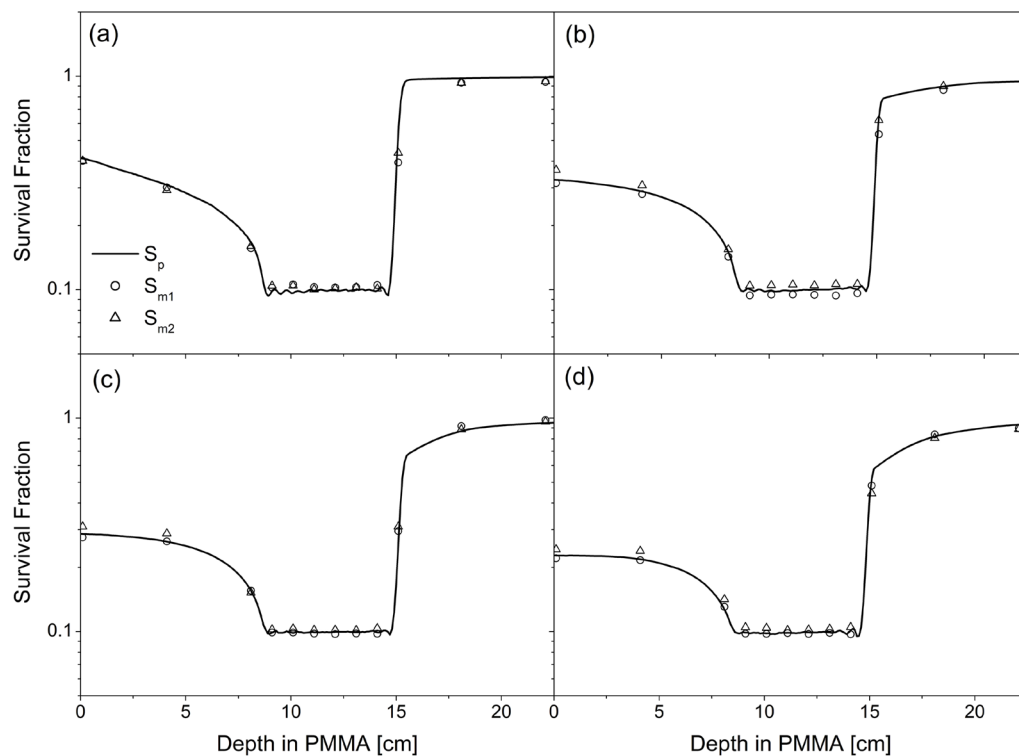


**Figure 4.** The measured survival fractions of HSGc-C5 cells (symbols) exposed to (a) helium-, (b) carbon-, (c) oxygen-, and (d) neon-ion fields as a function of depth in PMMA phantom, compared with the planned survival profiles based on the SMK model (solid curves). The survival fractions measured on different days are plotted with different symbols, i.e. open circles and open triangles.

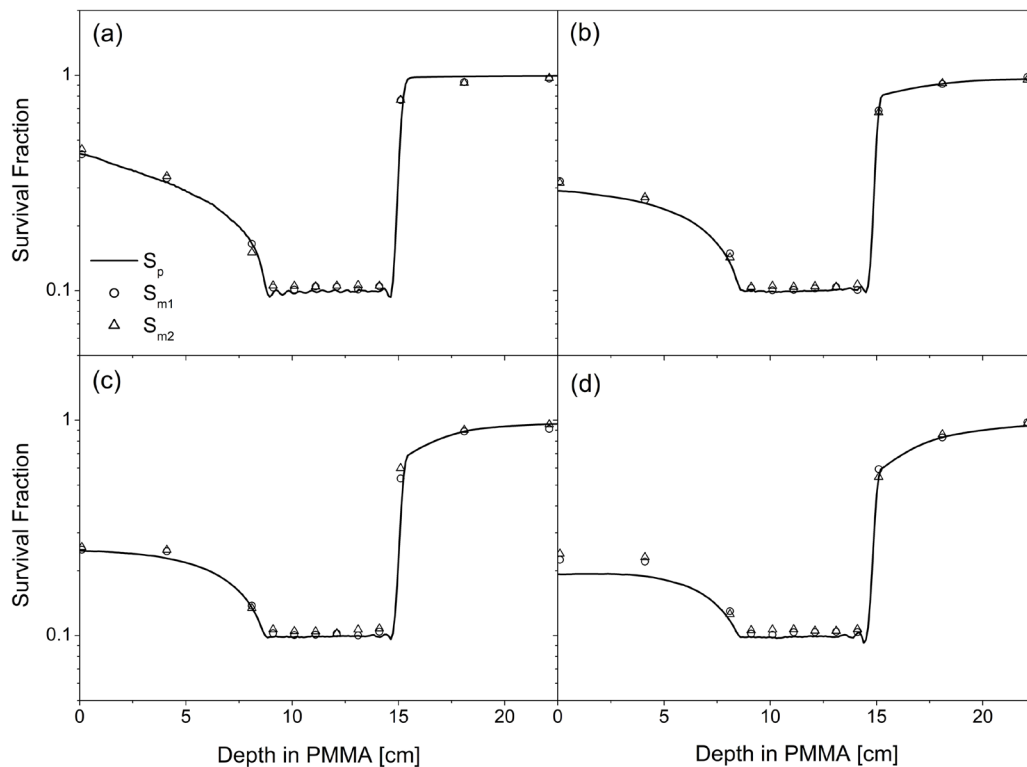
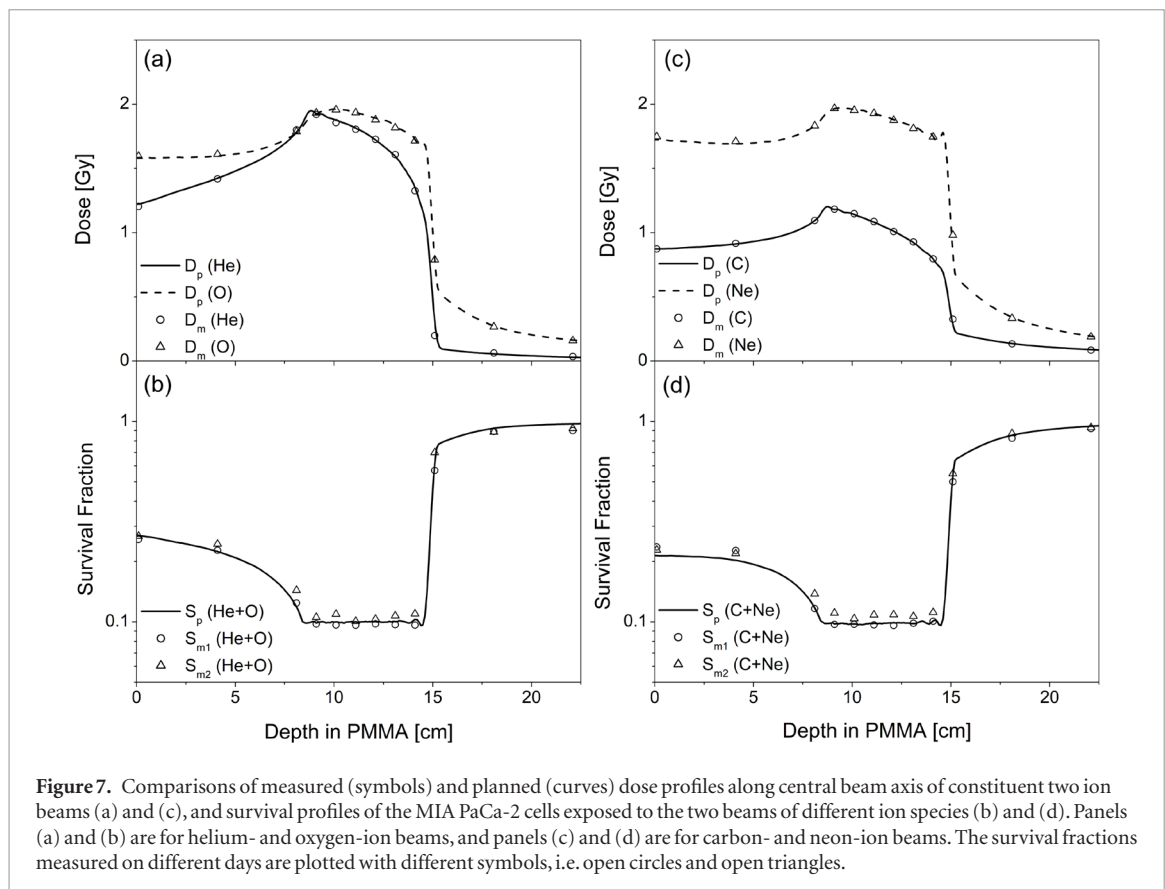
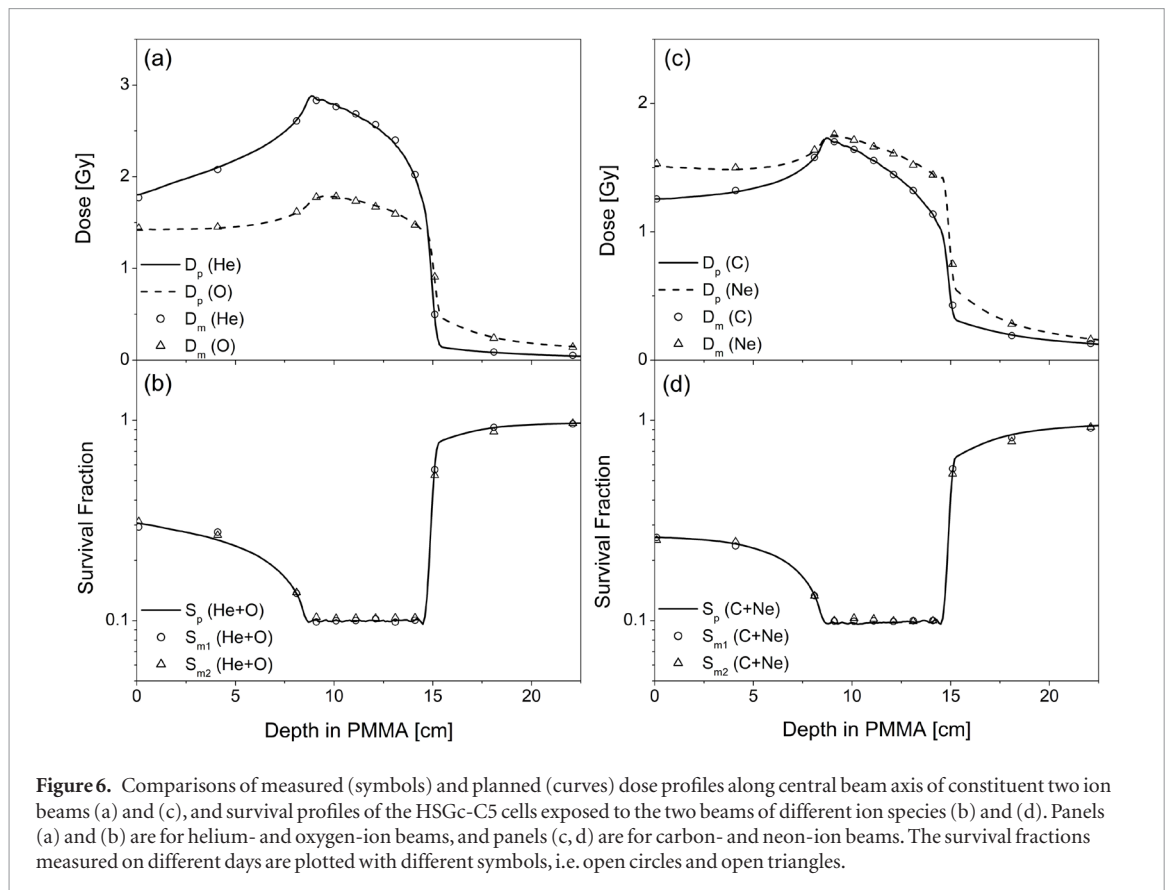


**Figure 5.** The measured survival fractions of MIA PaCa-2 cells (symbols) exposed to (a) helium-, (b) carbon-, (c) oxygen-, and (d) neon-ion fields as a function of depth in PMMA phantom, compared with the planned survival profiles based on the SMK model (solid curves). The survival fractions measured on different days are plotted with different symbols, i.e. open circles and open triangles.



was 4.04 Gy ( $\alpha_x = 0.331 \text{ Gy}^{-1}$ ,  $\beta_x = 0.0593 \text{ Gy}^{-2}$ ). This value was somewhat lower than the value of 4.80 Gy ( $\alpha_x = 0.252 \text{ Gy}^{-1}$ ,  $\beta_x = 0.0474 \text{ Gy}^{-2}$ ) measured during the period of this study (supplemental figure S1).

As shown in figures 4 and 5, the difference in survival fractions at the entrance and at the target was larger for lighter ions, showing the maximum in the helium ion beams for both cell lines. The helium-ion beam may be

superior to other heavier ion beams for controlling some human tumor cells under an aerobic condition (Burigo *et al* 2015). The heavier ions with high LET are, however, more effective to control radioresistant tumors under a hypoxic condition (Scifoni *et al* 2013, Hirayama *et al* 2015). Combining multiple ion species in accordance with the radiation sensitivity of tumors and surrounding risk organs will be useful to maximize the therapeutic effects of charged-particle beams. The SMK model can be used for treatment planning of hypo-fractionated multi-ion therapy with wide LET and dose ranges.

## 5. Conclusion

For the hypo-fractionated multi-ion therapy, we had previously developed the SMK model as an extension of the MK model clinically used in carbon-ion radiotherapy in Japan. In this study, we verified the SMK model for treatment planning of helium-, carbon-, oxygen-, and neon-ion beams as well as their combinations through cell irradiation experiments of two human cell lines. The survival fractions of the cells exposed to the pristine beams of four ion species at different LETs were measured by a colony-forming assay, and the SMK model parameters were determined for the cell lines. Treatment plans were made with the single-ion beams or combinations of the beams of two ion species to achieve a 10% survival of the cells within a cuboid target in a PMMA phantom. The planned survival profiles reasonably agreed with the measured survival fractions in the whole region from the plateau to the fragment tail for all planned irradiations. The difference between the corresponding x-ray doses averaged over the target and the prescribed dose was less than 1.5% for all plans. The SMK model offers the accuracy and simplicity required in multi-ion therapy treatment planning with wide LET and dose ranges.

## ORCID iDs

Nobuyuki Kanematsu  <https://orcid.org/0000-0002-2534-9933>

## References

- Agostinelli S *et al* 2003 Geant4—a simulation toolkit *Nucl. Instrum. Methods. Phys. Res. A* **506** 250–303
- Böhlen T T, Bauer J, Dosanjh M, Ferrari A, Heberer T, Parodi K, Patera V and Mairani A 2013 A Monte Carlo-based treatment-planning tool for ion beam therapy *J. Radiat. Res.* **54** i77–i81
- Böhlen T T, Brons S, Dosanjh M, Ferrari A, Fossati P, Heberer T, Patera V and Mairani A 2012 Investigating the robustness of ion beam therapy treatment plans to uncertainties in biological treatment parameters *Phys. Med. Biol.* **57** 7983–8004
- Burigo L, Pshenichnov I, Mishustin I and Bleicher M 2015 Comparative study of dose distributions and cell survival fractions for 1H, 4He, 12C and 16O beams using Geant4 and Microdosimetric Kinetic model *Phys. Med. Biol.* **60** 3313–32
- Chatterjee A and Schaefer H J 1976 Microdosimetric structure of heavy ion tracks in tissue *Radiat. Environ. Biophys.* **13** 215–27
- Chen Y, Li J, Li C, Qiu R and Wu Z 2018 A modified microdosimetric kinetic model for relative biological effectiveness calculation *Phys. Med. Biol.* **63** 015008
- Furukawa T *et al* 2010 Performance of the NIRS fast scanning system for heavy-ion radiotherapy *Med. Phys.* **37** 5672–82
- Furusawa Y, Fukutsu K, Aoki M, Itsukaichi H, Eguchi-Kasai K, Ohara H, Yatagai F, Kanai T and Ando K 2000 Inactivation of aerobic and hypoxic cells from three different cell lines by accelerated He-, C- and Ne-ion beams *Radiat. Res.* **154** 485–96
- Grün R, Friedrich T, Traneus E and Scholz M 2019 Is the dose-averaged LET a reliable predictor for the relative biological effectiveness? *Med. Phys.* **46** 1064–74
- Heberer T, Becher W, Schardt D and Kraft G 1993 Magnetic scanning system for heavy ion therapy *Nucl. Instrum. Methods Phys. Res. A* **330** 296–305
- Hada M and Georgakilas A G 2008 Formation of clustered DNA damage after high-LET irradiation: a review *J. Radiat. Res.* **49** 203–10
- Hawkins R B 1994 A statistical theory of cell killing by radiation of varying linear energy transfer *Radiat. Res.* **140** 347–66
- Hawkins R B 1996 A microdosimetric-kinetic model of cell death from exposure to ionizing radiation of any LET, with experimental and clinical applications *Int. J. Radiat. Biol.* **69** 739–55
- Hirayama R *et al* 2015 Determination of the relative biological effectiveness and oxygen enhancement ratio for micronuclei formation using high-LET radiation in solid tumor cells: an *in vitro* and *in vivo* study *Mutat. Res.* **793** 41–7
- Inaniwa T and Kanematsu N 2015 A trichrome beam model for biological dose calculation in scanned carbon-ion radiotherapy treatment planning *Phys. Med. Biol.* **60** 437–51
- Inaniwa T and Kanematsu N 2018 Adaptation of stochastic microdosimetric kinetic model for charged-particle therapy treatment planning *Phys. Med. Biol.* **63** 095011
- Inaniwa T, Furukawa T, Kase Y, Matsufuji N, Toshito T, Matsumoto Y, Furusawa Y and Noda K 2010 Treatment planning for a scanned carbon ion beam with a modified microdosimetric kinetic model *Phys. Med. Biol.* **55** 6721–37
- Inaniwa T, Kanematsu N, Hara Y and Furukawa T 2015a Nuclear-interaction correction of integrated depth dose in carbon-ion radiotherapy treatment planning *Phys. Med. Biol.* **60** 421–35
- Inaniwa T, Kanematsu N, Hara Y, Furukawa T, Fukahori M, Nakao M and Shirai T 2014 Implementation of a triple Gaussian beam model with subdivision and redefinition against density heterogeneities in treatment planning for scanned carbon-ion radiotherapy *Phys. Med. Biol.* **59** 5361–86
- Inaniwa T, Kanematsu N, Matsufuji N, Kanai T, Shirai T, Noda K, Tsuji H, Kamada T and Tsujii H 2015b Reformulation of a clinical-dose system for carbon-ion radiotherapy treatment planning at the National Institute of Radiological Sciences, Japan *Phys. Med. Biol.* **60** 3271–86

- Inaniwa T, Kanematsu N, Noda K and Kamada T 2017 Treatment planning of intensity modulated composite particle therapy with dose and linear energy transfer optimization *Phys. Med. Biol.* **62** 5180–97
- Inaniwa T, Lee S H, Mizushima K, Sakata D, Iwata Y, Kanematsu N and Shirai T 2020 Nuclear-interaction correction for patient dose calculations in treatment planning of helium-, carbon-, oxygen-, and neon-ion beams *Phys. Med. Biol.* **65** 025004
- Inaniwa T, Suzuki M, Furukawa T, Kase Y, Kanematsu N, Shirai T and Hawkins R B 2013 Effects of dose-delivery time structure in biological effectiveness for therapeutic carbon-ion beams evaluated with microdosimetric kinetic model *Radiat. Res.* **180** 44–59
- Kanai T et al 1999 Biophysical characteristics of HIMAC clinical irradiation system for heavy-ion radiotherapy *Radiat. Res.* **44** 201–10
- Kanai T, Matsufuji N, Miyamoto T, Mizoe J, Kamada T, Tsuji H, Kato H, Baba M and Tsujii H 2006 Biophysical characteristics of HIMAC clinical irradiation system for heavy-ion radiotherapy *Int. J. Radiat. Oncol. Biol. Phys.* **64** 650–6
- Kase Y, Kanai T, Matsumoto Y, Furusawa Y, Okamoto H, Asaba T, Sakama M and Shinoda H 2006 Microdosimetric measurements and estimation of human cell survival for heavy-ion beams *Radiat. Res.* **166** 629–38
- Kiefer J and Straaten H 1986 A model of ion track structure based on classical collision dynamics *Phys. Med. Biol.* **31** 1201–9
- Krämer M and Scholz M 2000 Treatment planning for heavy-ion radiotherapy: calculation and optimization of biologically effective dose *Phys. Med. Biol.* **45** 3319–30
- Krämer M and Scholz M 2006 Rapid calculation of biological effects in ion radiotherapy *Phys. Med. Biol.* **51** 1959–70
- Krämer M, Scifoni E, Schmitz F, Sokol O and Durante M 2014 Overview of recent advances in treatment planning for ion beam radiotherapy *Eur. Phys. J. D* **68** 306
- Krämer M et al 2016 Helium ions for radiotherapy? physical and biological verifications of a novel treatment modality *Med. Phys.* **43** 1995–2004
- Kurz C, Mairani A and Parodi K 2012 First experimental-based characterization of oxygen ion beam depth dose distributions at the Heidelberg Ion-Beam Therapy Center *Phys. Med. Biol.* **57** 5017–34
- Manganaro L, Russo G, Cirio R, Dalmaso F, Giordanengo S, Monaco V, Muraro S, Sacchi R, Vignati A and Attali A 2017 A Monte Carlo approach to the microdosimetric kinetic model to account for dose rate time structure effects in ion beam therapy with application in treatment planning simulations *Med. Phys.* **44** 1577–89
- Miyamoto T et al 2003 Carbon ion radiotherapy for stage I non-small cell lung cancer *Radiother. Oncol.* **56** 127–40
- Sato T and Furusawa Y 2012 Cell survival fraction estimation based on the probability densities of domain and cell nucleus specific energies using improved microdosimetric kinetic models *Radiat. Res.* **178** 341–56
- Sato T, Watanabe R, Kase Y, Tsuruoka C, Suzuki M, Furusawa Y and Niita K 2011 Analysis of cell-survival fractions for heavy-ion irradiations based on microdosimetric kinetic model implemented in the particle and heavy ion transport code system *Radiat. Prot. Dosim.* **143** 491–6
- Scifoni E, Tinganelli W, Weyrather W K, Durante M, Maier A and Krämer M 2013 Including oxygen enhancement ratio in ion beam treatment planning: model implementation and experimental verification *Phys. Med. Biol.* **58** 3871–95
- Sokol O et al 2017 Oxygen beams for therapy: advanced biological treatment planning and experimental verification *Phys. Med. Biol.* **62** 7798–813
- Tessonnier T, Böhlen T T, Ceruti F, Ferrari A, Sala P, Brons S, Haberrer T, Debud J, Parodi K and Mairani A 2017b Dosimetric verification in water of a Monte Carlo treatment planning tool for proton, helium, carbon and oxygen ion beams at the Heidelberg Ion Beam Therapy Center *Phys. Med. Biol.* **62** 6579–94
- Tessonnier T, Mairani A, Brons S, Haberrer T, Debud J and Parodi K 2017a Experimental dosimetric comparison of 1H, 4He, 12C and 16O scanned ion beams *Phys. Med. Biol.* **62** 3958–82
- Tsujii H and Kamada T 2012 A review of update clinical results of carbon ion radiotherapy *Japan. J. Clin. Oncol.* **42** 670–85